Experimental and Theoretical Studies of Electrothermal Waves

ROBERT R. GILPIN* AND EDWARD E. ZUKOSKI†
California Institute of Technology, Pasadena, Calif.

Experimental and theoretical studies have been made of the electrothermal waves occurring in a nonequilibrium electrical discharge in a potassium-seeded argon plasma. The studies presented in this paper refer to discharges in transverse gas flow and magnetic field. The behavior of these discharges as determined by photographs, photomultiplier measurements, and voltage probes is discussed and the results interpreted in terms of a steady, one-dimensional theory. A single discharge was found to operate in one of three modes—the shorted, transition, or normal mode—depending on the length of the ionization transient. An extension of the one-dimensional theory to the inlet problem predicts the approximate length of this transient and thus provides criteria for the existence of each mode. The normal mode was studied in a duct with a series of circuits discharging in parallel across a gas flow. Here, a regular set of steady, one-dimensional streamers was found in the center of the duct between hot boundary regions along each electrode wall. The properties of the one-dimensional streamers are shown to agree in detail with values predicted from the one-dimensional theory. A scheme is then presented for calculation of the effective conductivity of a duct using the amplitude of conductivity fluctuations predicted by this theory.

Nomenclature

α = load factor of external circuit
β = Hall parameter
β_{crit} = Hall parameter at which instability occurs
γ = hot boundary region parameter
δ = thickness of hot boundary region
ϵ_{eo} = electron temperature in undisturbed case
$\varkappa$ = fraction of Joule heating going into ionization
λ = wavelength of steady disturbances
λ_o = wavelength of light at which heat transfer occurs
ν_{ee} = electron-electron collision frequency
$\Delta\nu$ = width of the resonant line
σ = electrical conductivity
σ_o = undisturbed electrical conductivity
σ_i = initial electrical conductivity
$\tilde{\sigma}$ = normalized electrical conductivity, σ/σ_o
σ_{BL} = boundary-region electrical conductivity
σ_{eff} = effective electrical conductivity
τ = time since formation of last streamer
τ_s = time of smooth rise of voltage
m_e = mass of the electron
m_o = reciprocal photon mean free path at line center
n = exponent of J in $\sigma(J)$ formula
n_e = electron density
n_{eo} = undisturbed electron density
r = resistance per unit length of a streamer
l_o = distance streamers form behind electrodes divided by v_g
v_g = gas velocity
w = duct width
x = distance measured upstream from old streamer
B_{oo} = blackbody radiation intensity
E_o = electric field along a streamer
E_{oi} = electric field along a streamer when it forms in inlet region
E_L = total electric field in undisturbed case
E_{Lo} = electric field along J in undisturbed case
H = heat-transfer term
I = effective conductivity parameter[8]
I_i = ionization potential of seed
I_{pre} = preionizing current
J_o = current density perpendicular to streamer
J_L = current density in undisturbed case
K = effective energy diffusion coefficient
Q = electronic heating term
R_{ex} = resistance in external circuit
S = mean square conductivity variation
$V_\perp$ = voltage perpendicular to gas flow
$V_\parallel$ = voltage parallel to gas flow

Received June 6, 1968; revision received February 17, 1969. This work was supported by the Air Force Office of Scientific Research under Contract AF 49(638)-1285.

* Graduate Student in Engineering Sciences, Daniel and Florence Guggenheim Jet Propulsion Center, Kármán Laboratory of Fluid Mechanics and Jet Propulsion; now at Institute for Aerospace Studies, University of Toronto, Toronto, Canada.

† Professor of Engineering and Jet Propulsion, Daniel and Florence Guggenheim Jet Propulsion Center, Kármán Laboratory of Fluid Mechanics and Jet Propulsion. Associate Fellow AIAA.

Introduction

THE present paper describes a study of electrothermal instabilities observed in a seeded plasma in which nonequilibrium ionization was important. These disturbances have been observed by a number of investigators,[4,9–11] and are due to the strong coupling between electric conductivity and heating of the electron gas. The effect of these instabilities is to reduce the effective electrical conductivity of the plasma. This reduction has been one of the primary means of identifying the presence of the phenomenon, and a large part of previous studies has been devoted to obtaining the influence of the various parameters of the system on the effective conductivity.

A previous paper[1] reported studies of the wavelike disturbance in a geometry designed to produce steady waves. In this paper, these studies have been extended to include an investigation of disturbances occurring in other geometric configurations, and the reduction of conductivity has been related to the measured characteristics of the disturbances. Voltage and light intensity measurements were used to construct a picture of the pattern of electric field and conductivity variations as a function of magnetic field strength and applied voltage.

Under some circumstances, these patterns were steady, and the characteristics of these disturbances could be compared with the theoretical predictions based on the model discussed in Ref. 1. However, it was necessary to extend the model to

include a description of the nonsteady phenomena which occur in the inlet region.

After a brief review of the theoretical work, discussed in detail in Refs. 1 and 15, experimental results are presented and related to the model.

Theory

In Ref. 1, the energy equation for a one-dimensional nonuniformity in electron density was obtained. This equation was of the form

$$I_i \frac{\partial n_e}{\partial t} + \frac{a}{n_e}\frac{\partial n_e}{\partial x} - H = Q(n_e) \tag{1}$$

where Q (the electronic heating term) is

$$Q = \sigma_o E_{Lo}{}^2\left[\tilde{\sigma}\left(\frac{E_o}{E_{Lo}}\right)^2 + 2\beta\left(\frac{J_o}{\sigma_o E_{Lo}}\right)\left(\frac{E_o}{E_{Lo}}\right) + \frac{1+\beta^2}{\tilde{\sigma}}\left(\frac{J_o}{\sigma_o E_{Lo}}\right)^2 - \sigma^{(2/n-1)}\right]$$

$$\frac{J_o}{\sigma_o E_{Lo}} = \frac{-\beta + [(1+\beta^2)(E_{Lo}/E_o)^2 - 1]^{1/2}}{1+\beta^2}\left(\frac{E_o}{E_{Lo}}\right)$$

and

$$\tilde{\sigma} = \sigma/\sigma_o = (J/J_L)^n$$

Note that Q accounts for Joule heating (first three terms) and elastic collision losses (the last term). The term H in Eq. (1) includes both radiative and electronic heat transfer and in Ref. 1 was approximated by the operator $K(d^2n_e/dx^2)$. However, most of the important quantitative results obtained from Eq. (1) are dependent primarily on the heating term Q and thus are independent of this approximation. Q has been normalized by the Joule heating $\sigma_o E_{Lo}{}^2$ for the uniform solution and is plotted in Fig. 1. Here, the effect of the angle that the σ perturbation has relative to the vector J for a uniform solution is included in the parameter E_{Lo}/E_o. This is the ratio of the electric field along J in the undisturbed case E_{Lo} to the field along the perturbation E_o. These parameters are shown schematically in the upper part of Fig. 1.

The Hall parameter β also has an important effect on the shape of the curves of Q vs σ. For a value of β less than that at which the instability occurs, β_{crit}, the slope of Q vs σ at σ_o is negative; however, for certain values of E_{Lo}/E_o, the absolute value of the slope is less than that occurring for $\beta = 0$. This means that the perturbations, such as those introduced by the electrodes, take longer to disperse when β is nonzero.

For $\beta > \beta_{\text{crit}}$, the slope of Q for certain values of E_{Lo}/E_o becomes positive at σ_o, and this indicates that σ_o is an unstable solution. However, zeros of Q which are stable points do occur for values of σ on either side of $\sigma = \sigma_o$, and these zeros determine the regime of instability plotted in Fig. 8. Thus, if one considers the growth of a streamer from a small disturbance, these zeros determine the maximum possible conductivity variations that can occur, in either the steady or unsteady case (some unsteady cases have been studied by Velikov[4] and also by Solbes[5]). If the streamers are steady, their maximum amplitude is determined by the nearest zero of Q and their shape and half-width are determined by heat transport processes, that is, $H = Q$. However, their amplitude will be somewhat less than the maximum allowed by the instability regime due to the damping effect of this heat transport. For small-amplitude waves, the heat transport was treated by Lutz,[12] from which an expression for the wavelength λ of steady sinusoidal disturbances can be obtained

$$\omega_e(2\pi/\lambda)^2 + \omega_R(2\pi/\lambda)^{1/2} = (dQ/d\sigma)|_{\sigma_0}$$

where the damping due to conduction is

$$\omega_e = \frac{4}{3}\frac{\epsilon_{eo}{}^3 n_{eo}}{(1+\beta^2)I_i m_e \nu_{ee}\sigma_o E_{Lo}{}^2}$$

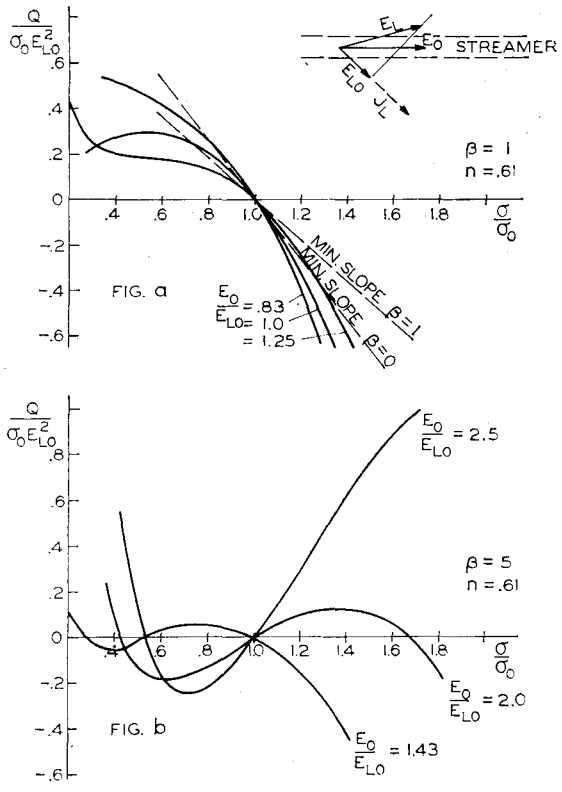

Fig. 1 The electronic heating term.

the damping due to radiation is

$$\omega_R = \frac{8(2)^{1/2}}{9}\pi^2\left[\frac{1.24\times10^4}{I_i\lambda_o}\right]\frac{\Delta\nu(m_o)^{1/2}B_{oo}}{\sigma_o E_{Lo}{}^2}$$

and the slope of Q vs σ at σ_o is

$$\left.\frac{dQ}{d\sigma}\right|_{\sigma_0} = \left(\frac{E_o}{E_{Lo}}\right)^2 - (1+\beta^2)\left(\frac{J_o}{\sigma_o E_{Lo}}\right)^2 - \left(\frac{2}{n}-1\right)$$

For the conditions occurring in the experiments, it was shown in Ref. 1 that as the amplitude increased, the width of the high-conductivity region, i.e., the streamer, did not increase much from $\lambda/2$; however, the spacing between streamers increased from $\lambda/2$ to ∞ as the amplitude increased. When spacing between the streamers is much greater than $\lambda/2$, considerations other than amplitude are likely to determine this spacing. Such a case occurs with a single discharge transverse to the gas flow, and this problem is discussed in the "Inlet" section of this paper.

Apparatus

The equipment used to generate the argon-potassium vapor mixture, which is the working fluid in these experiments, has been described in detail in Ref. 3. In the present work, the major change has been the use of a larger plenum chamber, 2.5-cm diameter, upstream of the test section, and of a smoothly contoured entrance between the plenum chamber and the rectangular test section. The test section is 2 cm high by 1 cm wide by 10 cm long. The magnetic field is applied parallel to the 1-cm dimension. The walls are boron nitride, and the electrodes and probes are tungsten rods, 0.075 cm and 0.05 cm, respectively. The working fluid is argon seeded with 0.2 mole % potassium, and at the test section entrance it has a uniform velocity profile, a speed of 100 m/sec, a temperature of 2000° ± 20°K, and a pressure of 1 atm. Typical duct-electrode configurations and a schematic

a) $B = 0, I = 1.5$ amp per electrode pair

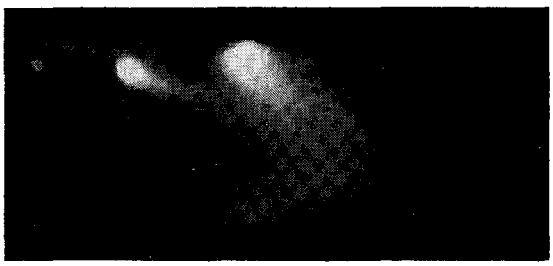

b) $B = 3$ kg, $I = 1.0$ amp per electrode pair

c) $B = 6$ kg, $I = 0.8$ amp per electrode pair

Fig. 2 Effect of magnetic field on inlet to a discharge region.

diagram of the electric circuit are shown in Figs. 3 and 7. Note that for present experiments UB is always less than 1 v/cm, and the reported values of the electric field are $(E - U \times B)$.

One of the 2-cm-high side walls was equipped with a quartz window through which optical observations were made by direct photography. In addition, light intensity measurements were made directly through small holes in the side walls; these holes were purged with a very small flow of argon during the tests. A lens and aperture system, giving a resolution in the duct of 0.05 cm, focused the light from the holes on plastic light pipes which carried the light signals to photomultiplier tubes. The light intensity has been shown[15] to be roughly proportional to the local conductivity; hence, the photomultiplier measurements can be used to obtain a quantitative picture of the average conductivity along a line of sight.

In some of the experiments, a preionizer was used to increase the electron density upstream of the first electrode pair. This consisted either of a pair of electrodes discharging parallel to the magnetic field or a device similar to that used by Evans,[14] in which case a 0.10-cm-diam ceramic tube spanning the 2-cm dimension of the duct was located just upstream of a regular electrode pair. The fluid-dynamic wake of this rod had no observable influence on the electrical phenomena occurring downstream; however, it did aid in igniting the first electrode pair. The test electrodes were located from 2 to 4 cm downstream of the preionizer.

Inlet

Photographs of the inlet to a duct with a series of discharges transverse to the gas flow showed (Fig. 2) that, as the magnetic field was increased while holding the current fixed, the discharge appeared to move farther downstream in the duct. For large β, the bright region of the discharge (and hence regions of large conductivity and current density) would be several duct widths behind the initial electrode pair. Also it was observed that luminous layers extended back from the electrodes along the electrode wall. In order to hold the current constant as β increased, it was necessary to decrease the resistance in the external circuit. When β was increased without holding the current constant, the light coming from the center of the duct moved back and decreased until only the glow along each electrode wall was seen. Alternatively, if the applied voltage was increased for a constant β, the transverse part of the discharge moved closer to the upstream electrode pair until it appeared between them. This last condition also could be produced by adding a preionizing discharge upstream of the test area.

Thus, there were three modes of operation that could be distinguished on the basis of the length of duct required for the ionization transient. In the first mode, where light is emitted only from the gas along the electrode walls, the transient length is larger than the test section length, and the entire duct operates in the shorted mode, as described by Kerrebrock.[2] In the second mode, light appears in the center of the duct but considerably downstream of the first electrode pair. This mode will be called the "transition" mode. In the third mode, the ionization length is short, and light is emitted the full length of the test section. This mode will be called the "normal" mode; however, it will be shown later that this mode is different than that described by Kerrebrock[2] in that the current is carried across the duct in a series of transverse streamers.

Qualitatively, the same modes of behavior occurred with a single transverse discharge: therefore, further study of the inlet problem was carried out with a single electrode pair. Also, since the shorted and normal modes are limits of the behavior observed in the transition mode, it was the transition mode that was studied in most detail.

Single Discharge in Cross Flow

In addition to visual observations, voltage and photomultiplier measurements were made in the region between the electrodes. Typical measurements made while the duct was operating in the transition mode are shown in Fig. 3. In this mode, the voltage between the transverse electrodes $V_\perp$ showed a sawtooth pattern. From the photomultiplier outputs L_1, L_2, and L_3 it can be seen that each sharp drop in the $V_\perp$ voltage is correlated with an increase in radiant energy which has been interpreted as the formation of a new streamer between the electrodes, and that a gradual increase of the $V_\perp$ voltage occurs as this streamer is being swept downstream with the gas. Also note that the Hall voltage $V_\parallel$ is very small during the gradual rise of the applied field (the amplification of $V_\parallel$ is twice that of $V_\perp$) and does not begin to rise until just before the formation of a new streamer. Correlation of arrival times from both light and voltage probes showed that streamers were transported by the gas and had negligible speeds relative to the gas.

From measurements of this type over a range of β, the following qualitative explanation of the inlet phenomenon was developed. As β increases from zero, nonuniformities introduced at the electrodes take longer to disperse and thus form high-conductivity paths along the electrode walls. These streamerlike paths tend to short out the Hall field, which, if entirely shorted out, would decrease the electronic heating rate for a given transverse field by a factor $1/(1 + \beta^2)$. This decrease in the electronic heating lengthens the ionization transient, thus shifting the discharge farther downstream. For $\beta > \beta_{crit}$, the transverse part of the discharge forms into a solitary streamer of the type described in Ref. 1. On either side of the streamer, the conductivity is at the lowest zero of Q; thus, there is no net electronic heating there. However,

as this streamer is carried downstream, the electric field between the electrodes rises. Note that in this experiment the maximum increase in the field is the battery source voltage divided by the electrode spacing. In a generator, the same increase in field would occur; however, there the maximum field would be the open-circuit electric field $U \times B$.

As a result of this increase in electric field, the ionization rate and thus the conductivity between the electrodes increases. When the conductivity has increased to approximately the mean value it had in the old streamer, an increase in Hall field must follow in order to maintain the continuity of current along the duct.

This can be seen by considering regions of high and low conductivity adjacent to each other, as depicted between the electrodes in Fig. 4. Except for small variations of β with σ, Ohm's law states that the vectors of the total current and electric field, J and E, are at a fixed angle to each other. Also, from the current continuity and the fact that the electric field is curl-free,[1] the component of current perpendicular to the conductivity interface, J_o, and the component of field parallel to the interface, E_o, must be the same in both regions. Thus, going from the low- to the high-conductivity region implies a rotation of the vectors J and E while the angle between them remains constant, and as well an increase in their magnitudes so as to satisfy the condition that E_o and J_o must remain unchanged. Looking at Fig. 4, it can be seen that these conditions can be satisfied only if the Hall field and the current parallel to the conductivity interface increase. Physically, this means that the Hall field across the high-conductivity region or streamer has increased in order to drive an increased amount of current along the streamer. The increase in Hall field and the current in the high-conductivity region in turn cause an increase in electronic heating, thus forming a feedback loop which causes the final very rapid rise of conductivity to form a new streamer. This is a good illustration of the basic feedback mechanism which causes the nonlinear electron heating term and is responsible for the electrothermal instability.

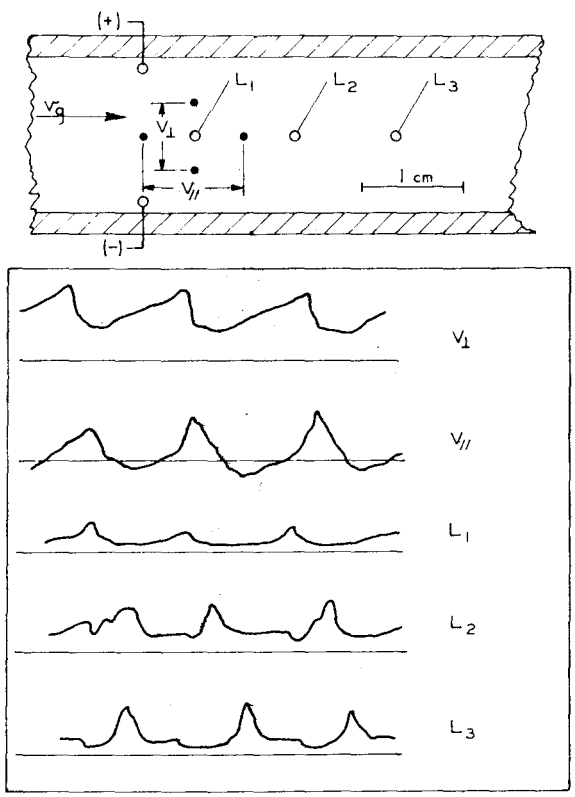

Fig. 3 Light and voltage measurements in inlet test section.

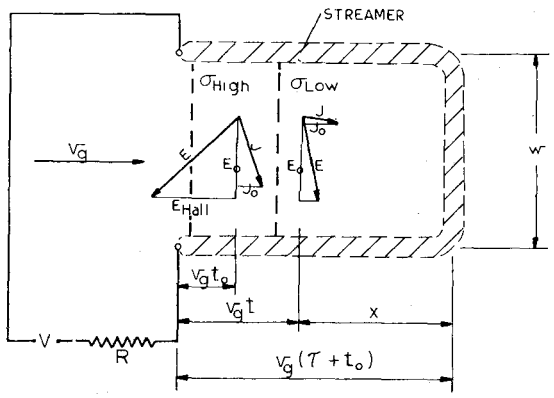

Fig. 4 Idealized inlet circuit.

In the inlet, the critical time in this process is the time required for the conductivity to be increased from the value entering the test section to the value at which the Hall field starts increasing. This time varies greatly with conditions in the duct and determines in which mode the duct will operate.

Calculation of Inlet Relaxation Length

The time required for the first phase of the stream production process can be calculated. Using the conditions existing during this phase, that is, Hall field zero and $\tilde{\sigma} = \sigma/\sigma_o < 1$, the energy equation is approximately

$$d\tilde{\sigma}/dt = \kappa(\tilde{\sigma}/n_{eo}I_i)\sigma_o E_o^2/[1 + \beta^2] \tag{2}$$

where the factor κ determines the fraction of the Joule heating that goes into ionization (the rest is radiated). For Eq. (2) with $\beta = 0$ to give the ionization rates measured by Cool,[3] the value 0.5 was given to κ. In Eq. (2), the effect of the magnetic field is that it reduces the Joule heating rate by the factor $1/(1 + \beta^2)$.

The electric field E_o is calculated for the idealized circuit shown in Fig. 4. Here, the old streamer is considered simply as a conducting path of constant resistance r per unit length, giving

$$E_o = E_{oi}\frac{1 + 2x/w}{1 + (2/w)\alpha(v_g t + x)} \tag{3}$$

where

$$\alpha = \frac{r(w + 2v_g t_o)}{R_{ex} + r(w + 2v_g t_o)}$$

and E_{oi} is the field along the streamer when it first forms. Since α is also the ratio of the minimum voltage across the duct to the source voltage, it is approximately equal to the expected loading factor for a generator. Using Eq. (3) in (2) and integrating from the time a given slug of gas enters the electric field (which is assumed to start on a line between the electrodes) until it is at a point $v\tau - x$ behind the electrodes gives an equation for σ as a function of x at a time after the formation of the last streamer. $\sigma(x)$ has a maximum between the electrodes and the old streamer. The value of τ at which this maximum reaches σ_o is taken as the time τ_s for the smooth rise in voltage. Because of the E^2 dependence of the Joule heating term, the conductivity is rising rapidly when it crosses the value σ_o; thus, τ_s is not strongly dependent on the value of σ chosen. The parameter that determines how the electric field increases as the old streamer is blown downstream is the distance it has been blown $v_g\tau_s$ normalized by the duct width w. This parameter is plotted in Fig. 5a as a function of the reciprocal of the reduced Joule heating $(1 + \beta^2)/E_o^2$, and shows good agreement with the observed time for the smooth part of the voltage rise. In Fig. 5b, the total

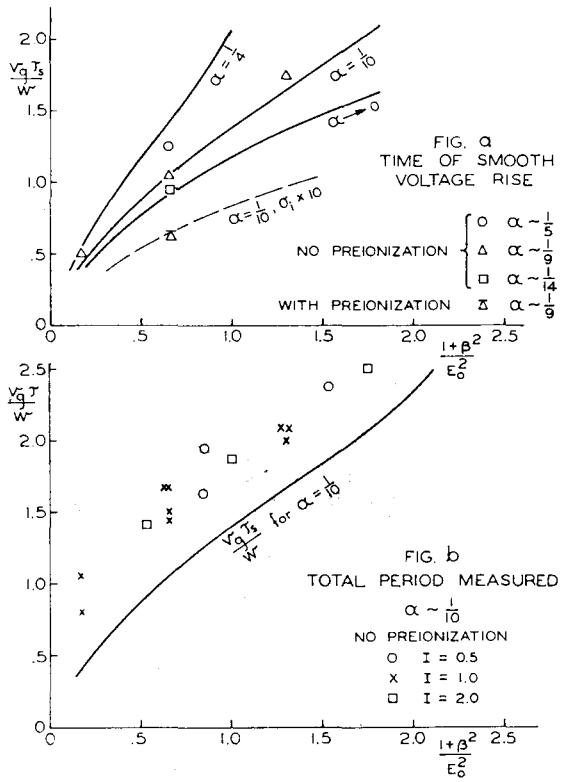

Fig. 5 Period of streamer formation in inlet region.

period of the streamers is plotted and compared to the theoretical value of $v_g\tau_s$. The difference between the two represents the time, in this case 50 to 100 μsec, required for the final growth of the new streamer and the associated drop of the duct voltage due to its shorting of the old streamer.

In Fig. 5a, note that for the curve $\alpha = \frac{1}{4}$ the value of the parameter $(v_g\tau_s)/w$, that is, the value of τ, rises increasingly rapidly for large τ. This is due to the fact that the voltage between the electrodes is approaching its maximum, which is the source voltage of the battery. From Eq. (3), setting $x = v_g\tau$ and $t = 0$, it can be seen that E_o has reached this limit for $2[(v_g\tau_s)/w] \gg 1/\alpha$. However, as this limit is approached, the field along the old streamer decreases rapidly, which may cause it to extinguish before a new streamer is formed. Experimentally, it was observed that for $2[(v_g\tau_s)/w] > 0.5(1/\alpha)$ the period of streamer formation became very erratic, and occasionally long periods occurred when the Hall field stayed near zero and no streamers appeared. That is, the duct was in the shorted mode.

In the other limit, when the distance $v_g\tau_s$ is less than the wavelength of steady disturbances, λ, the model again breaks down. Here, the distance between streamers is determined by the steady-state equation for the streamers, and the duct is then operating in the normal mode.

Prediction of the Mode of Operation

The condition $(2v_g\tau_s)/w < 0.5(1/\alpha)$ for a transverse streamer to form means that the circuit must be operating nearly as a constant current source. In the case $\alpha = 0$, that is, a constant current, the period is given explicitly by

$$\frac{2v_g\tau_s}{w} = \left[27\left(\ln\frac{\sigma_o}{\sigma_i}\right)\frac{v_g\tau_o}{w}(1+\beta^2)\right]^{1/3} - 1 \qquad (4)$$

where τ_o, the ionization parameter for $\beta = 0$, equals $(I_i n_{eo})/(\sigma_o E_o^2)$ (Ref. 3). This value of $(2v_g\tau_s)/w$ then can be used to predict which mode a given discharge will operate in. That is, if $(2v_g\tau_s)/w > 0.5(1/\alpha)$, the duct is shorted: if $2\lambda/w < (2v_g\tau_s)/w < 0.5(1/\alpha)$, the duct is in the transition mode and the length of the ionization region is $v_g\tau_s$; and if $(2v_g\tau_s)/w < 2\lambda/w$, the duct is in the normal mode.

Preionization

One way of decreasing $v_g\tau_s$ and thus producing the normal mode is to increase the initial value of the conductivity σ_i by preionization. In Fig. 6, the effect is shown of a preionizing discharge two duct widths upstream of the test electrode pair. As the preionizing current I_{pre} is increased, the time for the gradual rise of the voltage decreases to the point where the voltage is essentially constant and the streamers are close together. This set of streamers now looks much like those predicted by the periodic solution obtained in Ref. 1. Here, the distance between the streamers depends on their amplitude, and their maximum amplitude is fixed by the lowest zero of Q. A duct with a regular series of transverse streamers of this type has been defined here as operating in the normal mode.

The light intensity seen at the test section when only the preionizer was on is shown at the bottom of Fig. 6. From these measurements, σ_i with preionization was estimated to be 0.1 to 0.2 of σ_o, which was 1.5 mho/cm. However, this is an increase of about a factor of 10 over the σ_i without preionization, which is the equilibrium value of 0.03 mho/cm for this plasma. In Fig. 5, the calculated effect on $v_g\tau_s$ of a factor of 10 increase in σ_i is shown to be consistent with the observations.

Multiple Transverse Discharges

The normal mode of operation was studied in a duct with a series of circuits discharging in parallel across the test section. The test section for the multiple discharges had electrodes spaced every $\frac{1}{2}$ cm (see Fig. 7), which is less than the streamer spacing of 1 cm.

The development of the streamer pattern is shown in Fig. 7 as a function of β. As β was increased above the critical value of about 2, a set of regular streamers appeared (Fig. 7) of the same size and spacing as seen with a single preionized discharge (Fig. 6). The similarity of the two situations indicates that the upstream discharges act mainly as preionizers

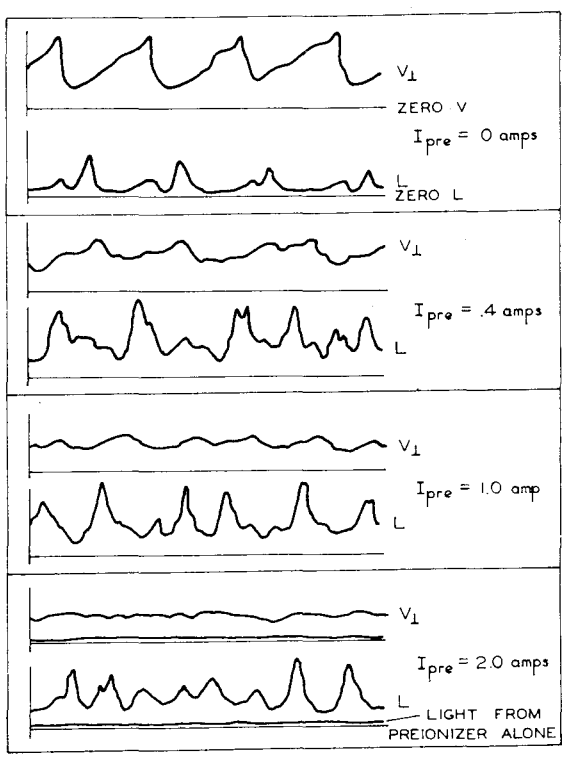

Fig. 6 Effect of preionization on a single discharge.

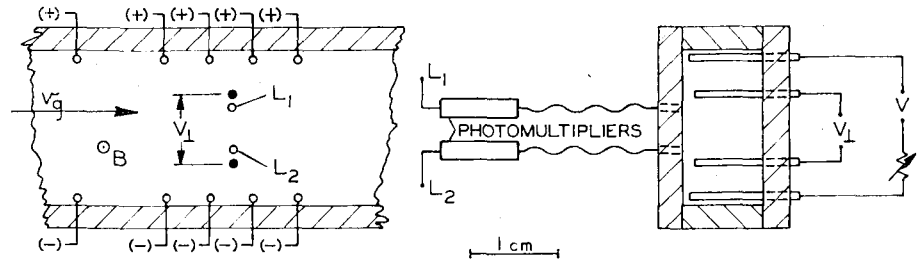

Fig. 7 Multiple transverse discharges.

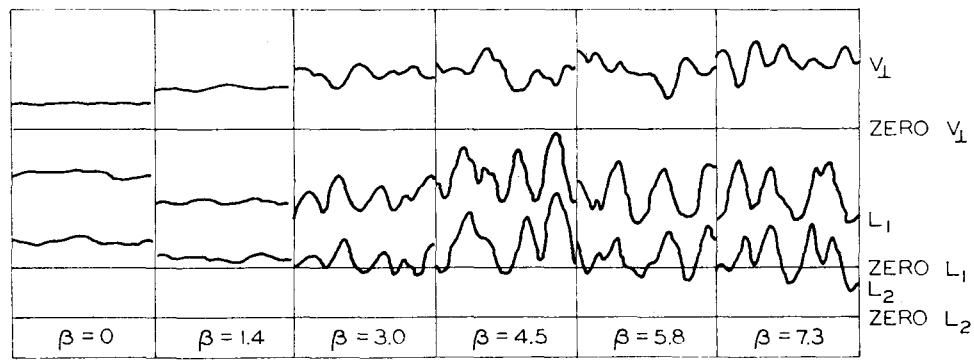

for the following ones. Detailed light probe measurements, e.g., L_1 and L_2 of Fig. 7, showed that the streamers were straight, one-dimensional disturbances which lay perpendicular to the gas velocity and were well defined to within 2 mm of the 0.75-mm-diam electrodes. A similar regular pattern of transverse streamers was observed by Zauderer[9] in high-speed photographs of a magnetohydrodynamic generator with a similar configuration of electrodes but with xenon gas as the working fluid. It is therefore expected that this is a practically important mode of operation.

In the experiments shown in Fig. 7, when β was increased from zero to 1.4, which is below the value at which the instability develops, the electric field increased and the light intensities decreased. This is due to the formation of higher conductivity zones along the electrode walls, as was predicted by Kerrebrock[2] for the shorted mode of a magnetohydrodynamic generator. These zones, also observed by Fischer,[13] are of the same origin as the streamers formed behind the electrodes in the case of a single discharge.

In Fig. 8, the conductivity and field fluctuations measured in the transverse streamers for $\beta = 4.5$ are shown to lie within the instability regime on a σ/σ_o vs E_{Lo}/E_o plot. In Fig. 9, the measured values of E_{Lo}/E_o are plotted as a function of β, and this diagram shows that the fluctuations lie in the instability regime over the whole range of β. For a constant current, note that E_{Lo} over E_o is the ratio of the perpendicular field measured with $\beta = 0$ to that when the magnetic field is applied. Conductivity nonuniformities occurring at higher values of β do cause a change in the average conductivity, and thus in E_{Lo}; however, the associated correction to E_{Lo} would be less than 5%.

From the steady theory, the maximum steady wave amplitude can be calculated as a function of wave angle, that is, of E_{Lo}/E_o; however, the angle, if any, at which steady waves will actually exist cannot be directly determined. To answer this problem analytically, a stability analysis of the steady waves must be done. This is very difficult to carry out in general; however, a simple analysis[15] suggests that the value of the effective Hall parameter defined in terms of average fields and currents should be a minimum to produce the most stable set of steady waves. This criterion is essentially the same as that used by Solbes.[5] In Fig. 9, it can be seen that the measured values of E_{Lo}/E_o are indeed scattered about the theoretical curve for minimum β_{eff}. Also note that all the values lie below the theoretical curve for the maximum possible amplitude waves. However, it also was found in Ref. 15 that a necessary condition for stability of an infinite plasma was that β_{eff} must be less than β_{crit}, and for theoretical values of β greater than about three, this condition was not produced by the predicted set of steady waves. The observation of apparently steady waves in this experiment up to theoretical Hall parameters of seven may be due to the stabilizing effect of the wall electrodes. That the walls may have had a stabilizing effect is indicated by the result discussed in Refs. 4 and 15, e.g., that in a test section with the electrodes many wavelengths away from the discharge, the steady streamers did become unstable for Hall parameters greater than three.

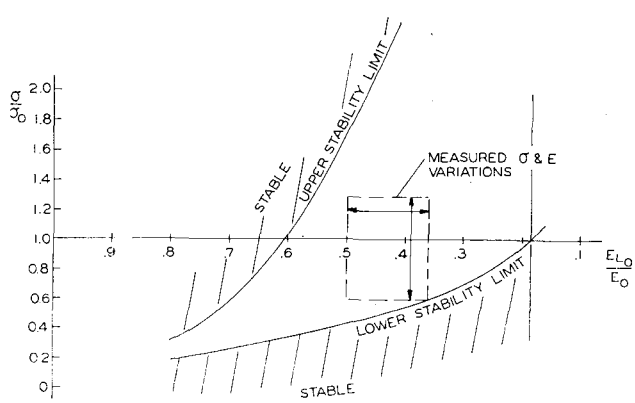

Fig. 8 σ and E variations measured in transverse streamers.

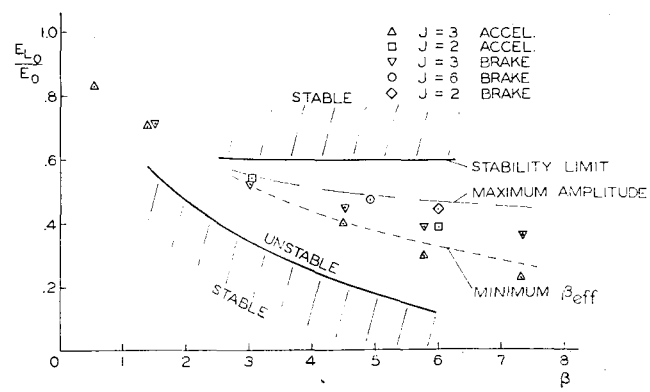

Fig. 9 Comparison of field along waves with field for unstable region.

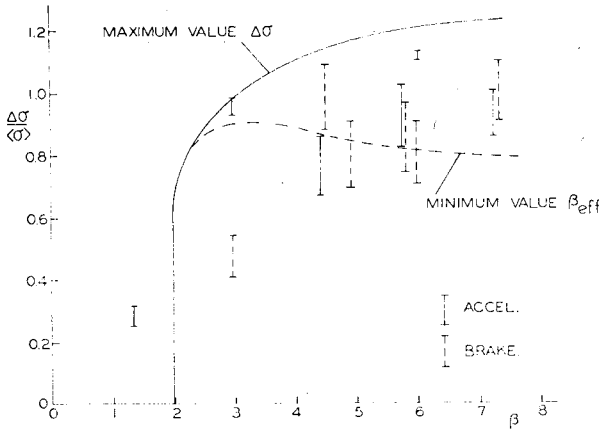

Fig. 10 Comparison of $\Delta\sigma/\langle\sigma\rangle$ with theory.

However, since the transverse streamers here are one-dimensional and steady, it is possible to use the model of Ref. 1 to calculate the approximate peak-to-peak conductivity variation $\Delta\sigma$ occurring in the duct. This $\Delta\sigma$ then can be used to predict the effective conductivity of the plasma.

Calculations of $\Delta\sigma$

Theoretically, for steady waves, the nearest zero of Q (Fig 8) fixes the maximum amplitude for a given value of E_{Lo}/E_o. In the region on this plot from $E_{Lo}/E_o = 0.52$ to 0.2, the lower zero fixes the amplitude and from $E_{Lo}/E_o = 0.61$ to 0.52, the upper zero does. Since the maximum variation occurs when the two zeros are equidistant, it follows that if E_{Lo}/E_o is allowed to vary, the true maximum peak-to-peak amplitude is the difference in conductivity between the upper and lower zeros occurring when $E_{Lo}/E_o = 0.52$. For this case, $\Delta\sigma/\langle\sigma\rangle = 1.2$. This was the criterion used to obtain the upper curve in Fig. 10.

Measured values of $\Delta\sigma/\langle\sigma\rangle$ lie below this maximum possible amplitude, and in the range of the value for waves that give minimum β_{eff}, the dashed curve in Fig. 10. The values of $\Delta\sigma/\langle\sigma\rangle$ for minimum β_{eff} are also very similar to those calculated by Solbes[5] using a different approach.

These results were essentially independent of the direction of the $J \times B$ force relative to the gas velocity, that is, whether the duct was accelerating or braking the gas flow. However, $\Delta\sigma$ is dependent on n, the exponent of J in the $\sigma(J)$ formula. The value $n = 0.61$ was chosen to agree with the σ vs J curve measured by Cool.[3]

Effective Conductivity in the Normal Mode

In these experiments, the transverse current was held constant as β was increased; therefore, E_{Lo}/E_o is equal to the ratio of the effective conductivity σ_{eff} to the conductivity σ_o with $\beta = 0$. To show that the measured σ_{eff} is consistent with the observed amplitude and pattern of conductivity fluctuations, a calculation of the effective conductivity was made for a duct with hot boundary regions on either side of a region with transverse conducting paths. This was done by calculating average fields and currents in each region from an analysis similar to Rosa's[6] and matching them across the division between the two regions. This analysis gives a relationship between σ_{eff} and $\langle\sigma\rangle$. By averaging the energy equation,[15] an approximate relation between $\langle\sigma\rangle$ and σ_o can then be obtained,

$$\langle\sigma\rangle/\sigma_o = \{(\sigma_{\text{eff}}/\sigma_o)[1 + \tfrac{1}{2}(2/n - 1)(2/n - 2)S]\}^{1/(1-2/n)} \quad (5)$$

where n is the exponent in the σ vs J relation. Using these two expressions and the fact that n was approximately $\frac{2}{3}$ in these experiments gives

$$\frac{\sigma_{\text{eff}}}{\sigma_o} = \left[\frac{\gamma + 1/(1 - \langle\sigma\rangle/\sigma_{BL})S\beta^2}{(\gamma + \beta^2)(1 + S)^{1/2}}\right]^{2/3} \quad (6)$$

where γ specifies the effective boundary region and is equal to

$$\gamma = 1 + (w/\delta)[1/(\sigma_{BL}/\langle\sigma\rangle - 1)]$$

Here, w is the width of the duct, δ is the width of the hot boundary region, and σ_{BL} is the average conductivity of the boundary. S is the mean square deviation for a sine wave of the normalized peak-to-peak amplitude plotted in Fig. 10. With no transverse streamers, that is, with $\Delta\sigma/\langle\sigma\rangle = 0$, the σ_{eff} would decrease along the curve marked 1-D in Fig. 11. This curve gives the effective conductivity for one-dimensional nonuniformities parallel to the flow and the magnetic field. The actual data lie considerably above this curve, due to the beneficial effect of the transverse streamers. The solid curves in Fig. 11 show the σ_{eff} calculated from Eq. (6) with $S = 0.125$, that is, for $\Delta\sigma/\langle\sigma\rangle = 1.0$ and for $\gamma = 3.0$ and 5.0. Most of the data are contained in this range of γ, which corresponds to two boundary regions, each of thickness 0.5 cm and having a conductivity 1.5 to 2.0 times that in the mainstream. These values are consistent with estimates that could be made from photographs of the duct. However, γ, generally, cannot be calculated with any degree of accuracy, and therefore only S is known.

Louis[7] has suggested that even though the actual conductivity nonuniformities may display distinct regularity, the effective conductivity might be predicted adequately by assuming an isotropic distribution of these nonuniformities. The calculation of σ_{eff} for such disturbances was made using the procedure of Yoshikawa and Rose.[8] This procedure accurately gives the effect of superposition of waves only for small-amplitude disturbances[16]; however, it may give an estimate of the effect of larger disturbances.

The procedure was also modified somewhat by using the assumption that the collision frequency was constant rather than the assumption, used earlier, that it was dominated by Coulomb collisions. Although this assumption is closer to the condition of this experiment, it does not change the result significantly. From this calculation, again correcting for the change of $\langle\sigma\rangle$,

$$\frac{\sigma_{\text{eff}}}{\sigma_o} = \left\{\frac{1 + (SI)^2 - 2SI/\beta + (SI/\beta)^2}{[1 - (1/\beta)SI + \beta SI](1 + S)^{1/2}}\right\}^{2/3} \quad (7)$$

where I, as defined in Ref. 15, goes to $\pi/4$ for large β and S is the mean square deviation of the conductivity. Equation (7) gives the curve marked 3-D in Fig. 11, where $S = 0.125$. This curve was too high; however, when the calculation of Ref. 8 was reformulated such that only isotropic conductivity fluctuations in the two dimensions perpendicular to the mag-

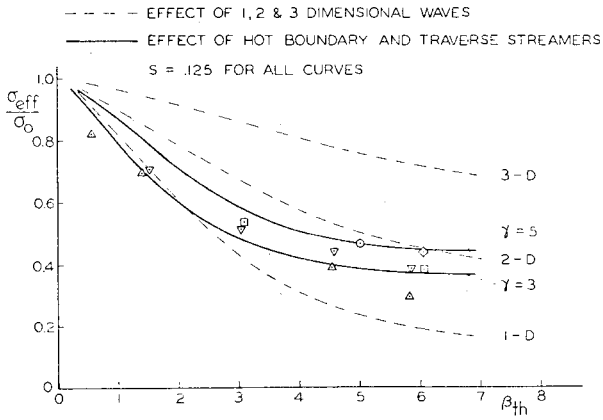

Fig. 11 Comparison of measured σ_{eff} with that for various patterns of nonuniformities.

netic field are allowed, better agreement was obtained. Here, the equation for σ_{eff} is

$$\frac{\sigma_{eff}}{\sigma_o} = \left\{ \frac{1 - S + (S^2/4)\beta^2}{[1 - S/2 + (S/2)\beta^2](1 + S)^{1/2}} \right\}^{2/3} \quad (8)$$

This result, marked 2-D in Fig. 11, agrees with the data at the higher values of β.

Conclusions

In a magnetic field, a single pair of electrodes discharging across a gas flow was observed to exhibit three qualitatively different modes of behavior: a shorted mode where high conductivity existed only along the electrode walls, a transition mode where transverse streamers were formed with a regular but large period, and a normal mode where the current was carried across the duct in a series of closely spaced streamers. There is a basic reason for the difference in behaviors of such a discharge with and without a magnetic field. With the magnetic field, regions of high conductivity along the walls, produced by current concentrations at the electrodes, short out the Hall field and hence decrease the Joule heating by a factor $1/(1 + \beta^2)$. Based on this concept, a simple theory of the inlet was developed from which the ratio of the length of the ionization zone to the duct width [i.e., $(v_g\tau_s)/w$] was calculated. Qualitatively, this parameter 1) increased with the ratio of final to initial conductivity, 2) increased with the parameter $(v_g\tau_o)/w$ where τ_o is the ionization parameter for $B = 0$, $(I_i n_{eo})/(\sigma_o E_o^2)$, and 3) increased with $(1 + \beta^2)$. The maximum length this ionization zone can have and still permit new streamers to be formed between the electrodes depends on the ratio of available source voltage to the duct voltage. That is, it depends on the load parameter of the circuit. When this limit is exceeded, the duct is in the shorted mode. In the other limit, when the ionization length is shorter than the wavelength of steady waves, the duct is in the normal mode.

For the practically important case of the inlet to a series of circuits discharging in parallel across a gas flow, that is, an accelerator or MHD generator, the situation is more complicated, and the criteria developed here will not be directly applicable. However, the qualitative effect of the various parameters will be the same, and the criterion for occurrence of the normal mode will probably still be valid.

The normal mode of operation was studied in detail in a duct with multiple transverse discharges. Here, it was observed that the light intensity pattern could be divided into two regions. The first is a hot boundary region along each electrode wall and the second is a region of steady, one-dimensional streamers transverse to the gas flow and lying between the hot wall layers.

The streamers in the center of the duct were studied in detail, and it was shown that their peak-to-peak amplitude, about 1.0 $\langle\sigma\rangle$ in this case, can be predicted by the steady, one-dimensional theory. Using the measured values for the streamers in the center of the duct and reasonable values for the boundary regions, the relative effect that the two regions have on the effective conductivity of the duct is shown. The hot boundary regions alone would have decreased the effective conductivity by a factor of 10 at $\beta = 5$; however, with the transverse streamers, the effective conductivity was decreased by a factor of 2.5 at the same β. The beneficial effect of operating a generator or accelerator in the normal mode is therefore obvious.

Since the characteristics of the boundary region would be difficult to calculate with any accuracy, a computational scheme was sought from which the effective conductivity could be derived using only the amplitude predicted by the steady theory. A model of a two-dimensional, isotropic distribution of conductivity nonuniformities of the predicted amplitude was found to give reasonable agreement with the measured values over the range of β considered.

References

[1] Zukoski, E. E. and Gilpin, R. R., "Large Amplitude Electrothermal Waves in a Nonequilibrium Plasma," *The Physics of Fluids*, Vol. 10, No. 9, Sept. 1967, pp. 1974–1977.

[2] Kerrebrock, J. L., "Segmented Losses in MHD Generators with Nonequilibrium Ionization," *AIAA Journal*, Vol. 4, No. 11, Nov. 1966, pp. 1938–1947.

[3] Cool, T. A. and Zukoski, E. E., "Recombination, Ionization, and Nonequilibrium Electrical Conductivity in Seeded Plasmas," *The Physics of Fluids*, Vol. 9, No. 4, April 1966, pp. 780–796.

[4] Velikhov, E. P., Dykhne, A. M., and Shipuk, I. Y., "Ionization Instability of a Plasma with Hot Electrons," *Proceedings of the VII International Conference on Phenomena in Ionized Gases*, Belgrade, 1965.

[5] Solbes, A., "Quasi-linear Plane Wave Study of Electrothermal Instabilities," *Proceedings of Symposium on MHD Power Generation*, Warsaw, 1968.

[6] Rosa, R. J., "The Hall and Ion Slip Effect in a Nonuniform Gas," Research Rept. 121, 1961, AVCO Corp.

[7] Louis, J. F., "Effective Ohm's Law in a Partially Ionized Plasma with Electron Density Fluctuations," *The Physics of Fluids*, Vol. 10, No. 9, Sept. 1967, pp. 2062–2065.

[8] Yoshikawa, S. and Rose, D., "Anomalous Diffusion of a Plasma Across a Magnetic Field," *The Physics of Fluids*, Vol. 5, 1962, pp. 334–340.

[9] Zauderer, B., "Convective and Lorentz Force Effects in a Linear, Supersonic Magnetohydrodynamic Channel," Paper 67-718, 1967, AIAA.

[10] Klepeis, J. and Rosa, R. J., "Experimental Studies of Strong Hall Effects and $U \times B$ Induced Ionization," *AIAA Journal*, Vol. 3, No. 9, Sept. 1965, pp. 1659–1666.

[11] Dethlefson, R. and Kerrebrock, J. L., "Experimental Investigation of Fluctuations in a Nonequilibrium MHD Plasma," *Proceedings of the 7th Symposium on Engineering Aspects of MHD*, Princeton, 1966.

[12] Lutz, M. A., "Radiation and Its Effects on the Nonequilibrium Properties of a Seeded Plasma," *AIAA Journal*, Vol. 5, No. 8, Aug. 1967, pp. 1416–1423.

[13] Fischer, F. W., "Experimentelle Untersuchungen der Stromdichteverteilung in einem Magnetohydrodynamischen Generator mit Segmentierten Elektroden," IPP 3/41, 1966, Institut für Plasmaphysik, Garching bei München.

[14] Evans, N. A., "Effect of Flow Velocity on a Single, Controlled Glow Discharge in Cesium-Seeded Argon," *AIAA Journal*, Vol. 5, No. 10, Oct. 1967, pp. 1908–1913.

[15] Gilpin, R. R., "Experimental and Theoretical Studies of the Electrothermal Waves in a Nonequilibrium Plasma," Ph.D. thesis, 1968, California Institute of Technology.

[16] Solbes, A., private communication.